



Original article

Adiantum capillus attained selenium nanoparticles (SeNPs) ameliorate resistive effects in rat model of gentamicin nephrotoxicity via regulation of Interlukin-1 β , tumor necrosis factor- α and engagement of Vimentin and Bcl-2 proteins

Sima Ahmad Najmaddin, Zahra Abdulqader Amin *

Pharmacognosy Department, College of Pharmacy, Hawler Medical University, Erbil 44001, Iraq



ARTICLE INFO

Article history:

Received 27 June 2022

Revised 24 November 2022

Accepted 20 December 2022

Available online 26 December 2022

Keywords:

Selenium

Adiantum capillus

Gentamicin

IL- β TNF- α

Bcl-2

Vimentin

ABSTRACT

In this study the green method for synthesizing selenium nanoparticles (SeNPs) is experienced, in which the leaf extract of *Adiantum capillus* was used as an effective chelating and capping agent for producing SeNPs. The characterization techniques that achieved to confirm the synthesis and the structure details of the SeNPs were: UV-Vis spectroscopy, FT-IR analysis, XRD, EDX and SEM analysis. The biological activity of the synthesized SeNPs were tested and compared to the crude extract of *Adiantum capillus* on gentamicin model of nephrotoxicity in Wistar rats. Sera were used to test the pro-inflammatory cytokines Tumor necrosis factor alpha (TNF- α) and Interleukin beta (IL- β) levels. Histopathology and immunohistochemistry analysis for the apoptosis regulator protein (Bcl-2) and the interstitial filament protein (Vimentin) were performed. Results revealed that the synthesized SeNPs peak appeared at 400–430 nm wave length with crystallite particle size is around 37 nm. The predominant shape is spherical and cubic at different magnification levels with a narrow size distribution of 22.04–128.43 nm. The synthesized SeNPs showed a strong protective effect against gentamicin induced toxic effects to the rat's kidneys obtained from the (kidney function parameters, histopathology evaluation, recovery of the pro-inflammatory cytokines IL- β and TNF- α level with retrieval of Bcl-2 and vimentin protein levels proximate to the vehicle control groups). Due to the significant protective effect of SeNPs, it considered much better than the crude extract of *Adiantum capillus* in the treatment of kidney injury; however, additional studies are necessary to find the precise mechanism of their action.

© 2022 The Author(s). Published by Elsevier B.V. on behalf of King Saud University. This is an open access article under the CC BY-NC-ND license (<http://creativecommons.org/licenses/by-nc-nd/4.0/>).

1. Introduction

In the recent years the synthesis of new nanoparticles from plant extracts have received a great attention from the researcher's worldwide through different application spectrums including medicinal, Food science and many agricultural technologies. Several methods and several metallic Nano-materials like (Gold, Silver, Zinc oxide, Selenium and Copper oxide) has been used for this pur-

pose, among these the sodium selenite (SeNPs) have been desired in many researches because of its extra-biological activities such as antioxidant (Shi et al., 2011; Han et al., 2017), antibacterial (Shoebi and Mashreghi, 2017; Ananth et al., 2019), anti-inflammatory (Lv et al., 2020) (Kim et al., 2021), prevention of cancer (Lipinski, 2017) (Wu et al., 2019) and many other biological and pharmacological effects (Pfister et al., 2016). On the other hand gentamicin is an aminoglycoside type of antibiotics, is well known for its nephrotoxicity effects by reducing the blood flow and glomerular filtration of the kidneys with rising the vascular resistance (Randjelovic et al., 2017). The gentamicin toxicity was reported to be through generating oxygen free radicals which in-turn damage the proximal tubules and increase the levels of urea and creatinine (Ali, 2004). Moreover, previous studies has proved that treatment with gentamicin cause an increase or imbalance in some pro-inflammatory cytokines stages like Interleukin-6 and tumor necrosis factor alpha (Erseçkin et al., 2020), interleukin-1 beta (Cao et al.,

* Corresponding author.

E-mail addresses: sima.najmaddin@pha.hmu.edu.krd (S A. Najmaddin), zahraa.alnajaar@hmu.edu.krd (Z A. Amin).

Peer review under responsibility of King Saud University.



Production and hosting by Elsevier

2019), Transforming growth factor beta (Bledsoe et al., 2006), the nuclear factor kappa-B and Interferon- gamma (Ince et al., 2020) and others. *Adiantum capillus* Linn. (*A. capillus*) is a tufted fern classified under Pteridaceae family it has been found to be effective against urinary tract infections (UTI) and some studies examined the anti-calcium oxalate urolithiasis activities of a hydroalcoholic extract of *A. capillus* in male rats. The obtained data indicated a considerable drop in the number of crystals and a lowering in calcium, phosphorous, and blood urea levels in the serum. Moreover, they verified this impact in an *in vitro* investigation. The plant stifled crystallization, aggregation, and a decrease in the number and size of crystals (Ahmed et al., 2013). The focal aim of the present study is to biosynthesize selenium nanoparticle from *Adiantum capillus* leaves and to study its ameliorative effect against gentamicin-induced toxicity to experimental rat's kidneys.

2. Materials and methods

The leaves of *Adiantum capillus* were air dried in the dark at room temperature, extracted, and mixed with sodium selenium solution. The synthesized (SeNPs) were characterized by (UV-visible) ultraviolet visible spectrophotometer, (FTIR) Fourier transform infrared spectrophotometer, (SEM) scanning electron microscopy and (EDX) energy-dispersive X-ray.

2.1. Crude plant extraction

The leaves were powdered then ten grams were added to 100 mL of distilled water and heated to 80 °C for thirty minutes. Settled suspension was filtered by Whatmann filter paper No. 40 (pore size 8 µm). To remove impurities, the filtered solution centrifuged at 4000 rpm for thirty minutes (Salari et al., 2019). The supernatant filtrated and concentrated using a rotary evaporator. The resultant crude extract was stored at 4°C for further use.

2.2. Synthesis of selenium nanoparticles (SeNPs)

Five milliliters of *Adiantum capillus* extract was diluted with 45 mL of 12 mM of Sodium selenite (Na_2SeO_3). The mix was stirred at 60 °C for three days until a yellow to ruby red color was seen. Then the product was washed with Deionized distilled water and centrifuge at 10,000 rpm for ten minutes (Pyrzynska and Sentkowska, 2021). Followed by a second washing of Phosphate buffer solution (pH 7.4) and ultra-sonication several times until

the impurities were removed. At the last, a light red pellet was dried in oven for two hours. and stored at -20 °C until use (Cittrarasu et al., 2021).

2.3. Field emission scanning electron microscopy and EDX

Field emission scanning electron microscopy was used to observe the morphology of synthesized SeNPs-A and its elemental composition.

2.4. UV-Visible spectroscopy

200–800 scan range and scan speed of 480 nm/min was used. The UV-vis absorption spectra of the SeNPs-A were recorded and plotted to numerical data using Microsoft Excel program.

2.5. FTIR

Translucent sample discs were prepared by encapsulating 2 mg of SeNPs-A in 100 mg potassium bromide pellet. Then prepared specimens were exposed to 400–4000 cm^{-1} (wavelength) with a 1 cm^{-1} (resolution) of Fourier transform infrared (FT-IR) spectroscopy.

2.6. XRD

Cu-K α radiation ($\lambda = 1.541 \text{ \AA}$ wavelength) was used to determine the crystalline size and purity by using Scherrer's equation ($D \cong 0.9\lambda/\beta \cos \theta$) where λ = wavelength of X-ray, D = crystal size, θ = Bragg angle in radians, and β is the full width at half maximum of the peak in radians.

2.7. Experimental animals

Forty-eight adult male Wistar rats weighing between (180–250 g) were used. Ethical principles of the National Institutes of Health's Guide for the Care and Use of Laboratory Animals were handled (Albus, 2012) (ethics number: 2022-8-25-212/HMU.PH.EC). The animals were separated into six groups (eight rats each) and the treatments were given for eight days.

Group I were injected with (100 mg/kg) gentamicin,

Group II were orally fed with normal saline,

Group III and IV were injected with (100 mg/kg) gentamicin and orally fed with 100 mg/kg and 200 mg/kg *A. capillus* crude extract,

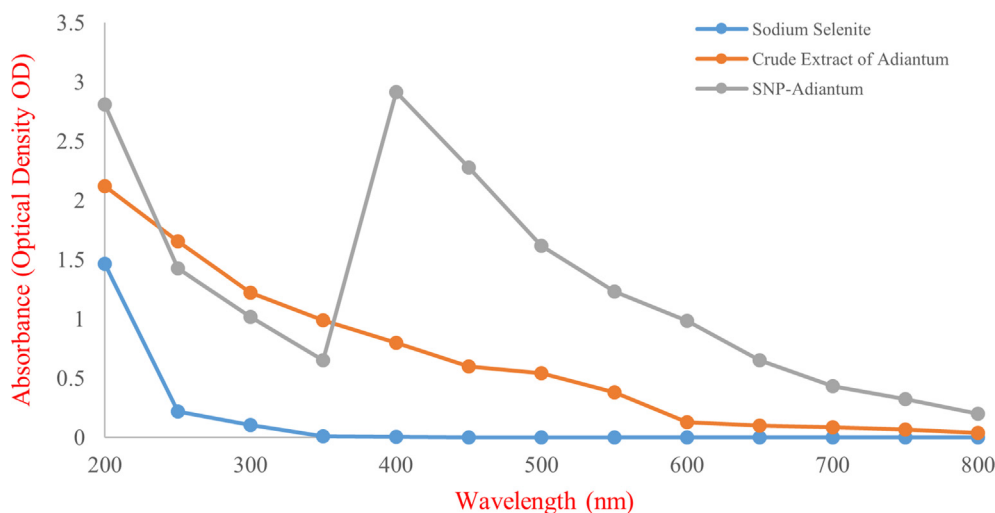


Fig. 1.

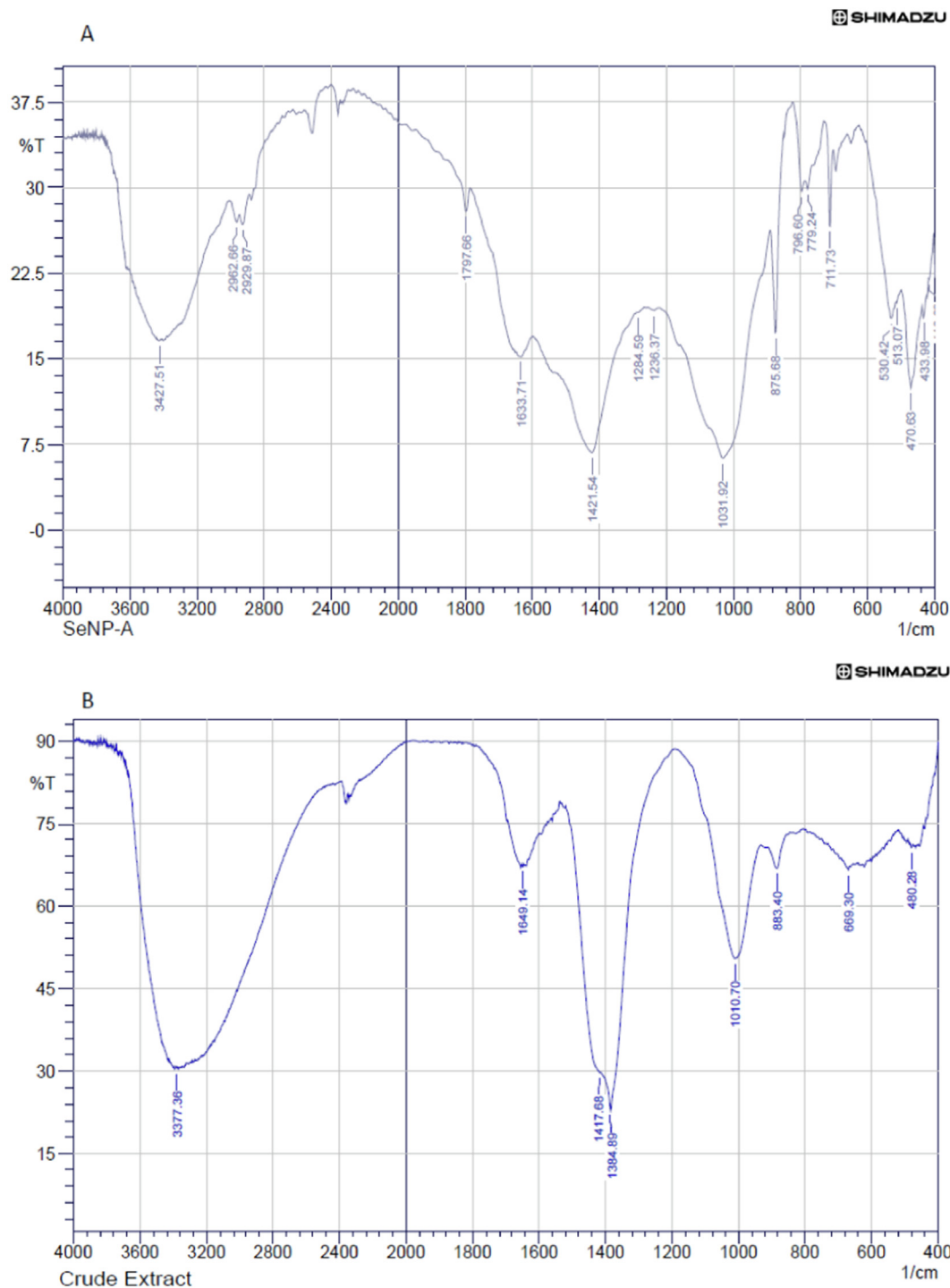


Fig. 2. FTIR analysis of SeNPs (a) and Crude extract of *A. capillus* (b). Different positions of several absorption peaks indicates the occurrence of many biomolecules on the surface of crude extract of *A. capillus* and SeNPs.

Group V and VI were injected with (100 mg/kg) gentamicin and orally fed with 100 mg/kg and 200 mg/kg SeNPs of *A. capillus* respectively.

Twenty-four hours after the eight-day experiment, ketamine (80 mg/kg) + xylazine (20 mg/kg) were injected intraperitoneally to anesthetize the animals' rats were sacrificed to obtain blood and kidney. An injector was driven to the left ventricle of the hearts of the anesthetized animals to draw the blood samples into the anticoagulant tubes (Uni-medica, China). Blood samples were cen-

trifuged at (4000 rpm for 10 min) to gain the serum used for serological and biochemical tests, kidney also obtained from each rats each sample were sectioned and placed in 10 % formalin. kidney biochemical parameters include: serum albumin (SA), creatinine (CR), blood urea nitrogen (BUN), albuminuria (AU), and uric acid (UA) with commercial kits (HITACHI, Germany) and using the COBAS 6000 machine (HITACHI, Germany). a second amount of rats sera were used to test the pro-inflammatory cytokines: tumor necrosis factor (TNF α) and interleukin (IL- β 1) levels by enzyme-

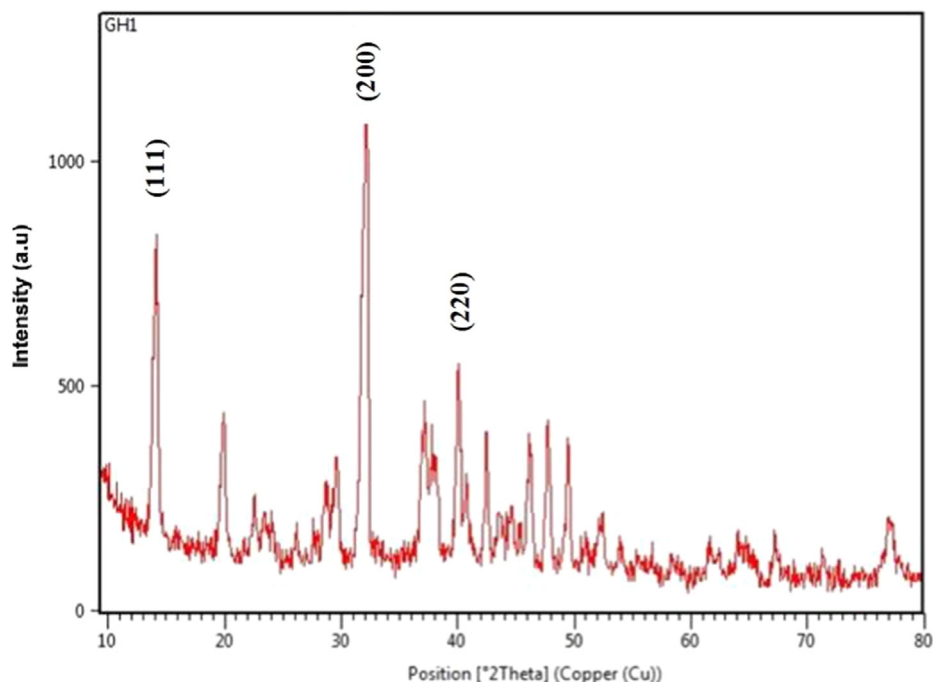


Fig. 3. *A. capillus* leaf extract synthesized selenium nanoparticle XRD spectrum.

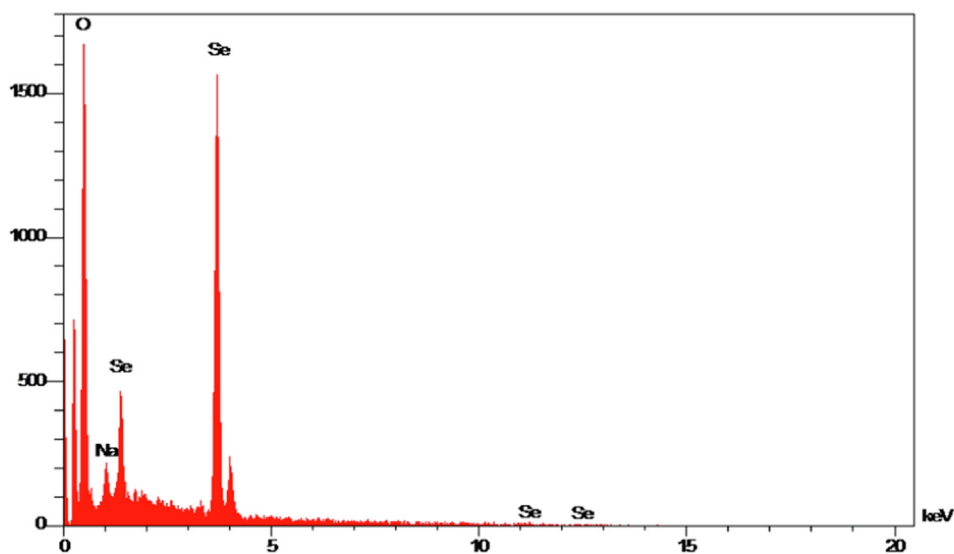


Fig. 4. EDX spectrum showing elemental composition analysis of SeNPs-A.

linked immunosorbent assay (ELISA) (Biochrom Anthos 2010, UK). The commercial kits were purchased from the Bioassay Technology Laboratory/Korea, for the detection of IL-1 β and TNF- α .

The excised kidney tissue was fixed with 10 % formalin solution for 48 hrs.(Erseçkin et al., 2020) and then subjected to a series of hydration and dehydration reactions with xylene and ethanol. Then the tissue is embedded with paraffin and sectioned into thin slices of about five-micron thickness using Microtome (semi-automated, HM 340E) (Thermo Scientific. USA). Tissue sections were stained with hematoxylin and eosin stain (Thermo Scientific. USA). The sections were viewed under a microscope (Olympus BX40, Japan) and photographed to analyze the histopathological changes in control and experimental rats (Zhang et al., 2019). Immunohistochemistry technique was used to determine nuclear

protein (Bcl-2) and kidney-specific antibody (Vimentin) in formalin-fixed kidney tissue specimens. The Bcl-2 antibody kit was acquired from (Genemed, Biotechnologies. Inc) and the Vimentin antibody kit was received from (Neo Genomics, USA), and the experiment was conducted following to the manufacturer's precise instructions and technique.

2.8. Statistical analysis

One-way ANOVA (analysis of variance), Post-Hoc Bonferroni test was used to set the significant differences between groups. A value of p -value < 0.05 was reflected the significance when compared to the control groups.

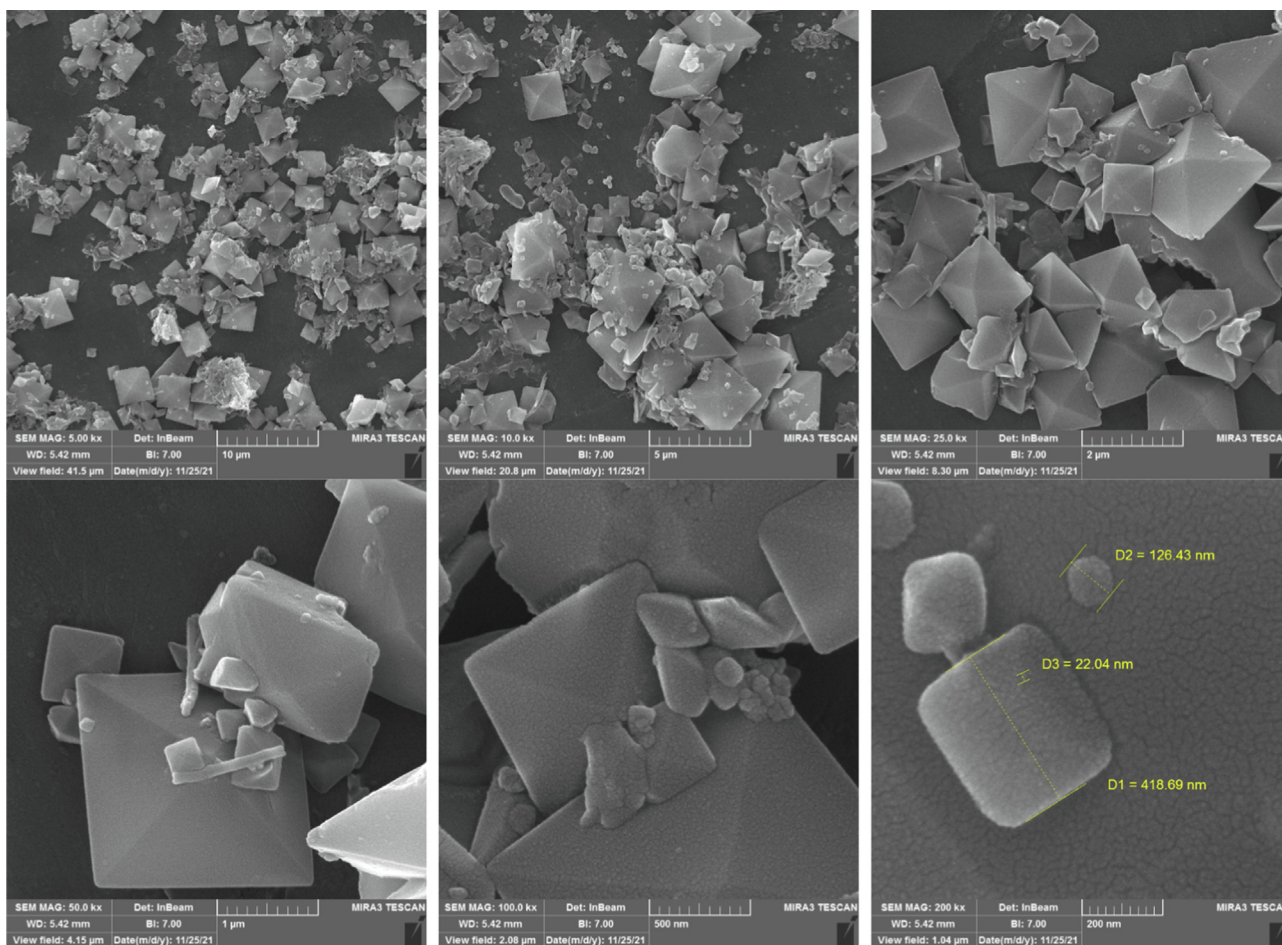


Fig. 5. Scanning electron microscopic micrographs of selenium nanoparticle (SeNPs) using *A. capillus* leaf extract at magnification of 200 mm (a), 500 mm (b), 1.0 µm (c), 2.0 µm (d), 5.0 µm (e) and 10 µm (f).

3. Results

3.1. Optical properties

Ultra-violet visible spectroscopy (wavelength between 200 and 800 nm) method was performed to screen the bio-synthesis of SeNPs. The newly synthesized SeNPs displayed high peaks of absorption about 2.5–2.9 (wavelength range between 400 and 430 nm) as shown in Fig. 1.

3.2. FTIR spectral analysis

The FTIR spectroscopic design was achieved to illustrate the functional groups existent in the colloidal form of SeNPs. The functional groups elaborate in reducing sodium selenite into SeNPs were assessed through FTIR spectroscopy of the synthesized SeNPs. Absorbance analysis of Infrared (IFR) radiations in ranges of 400–3500 cm^{-1} was tested for the samples (Fig. 2). The produced SeNPs showed two ranges peaks (400–1800 cm^{-1} and 2800–3500 cm^{-1}). The peaks of absorbance between 3200 and 3500 cm^{-1} definite the occurrence of O–H bonded strong and stretching vibrations because of the phenol and alcohol functional groups. Same for peaks region of 1600–1700 cm^{-1} , C=C stretching. Also the bio-synthesized SeNPs showed peaks at 1635.52 cm^{-1} and 3454.3 cm^{-1} . The peak between 2900 and 3200 cm^{-1} denoted the O–H vibrations while the peak between 1600 and 1700 cm^{-1} denoted the amide group.

Other two focal peaks were identified at 3427.51 cm^{-1} and 1633.71 cm^{-1} , which were correlated to hydroxyl and amide groups stretching vibrations respectively. Hydroxyl group is a strategic factor in the reduction process of selenium ions to their subsequent element. They can be as flavonoids, tannins and phenolic acid structures obtained from *A. capillus* extract. Oppositely, amide groups are important in the stabilizing of the SeNPs formed which occur as enzymes and proteins structures from *A. capillus*. The pH of *A. capillus* extract was around 5.0 which indicate the acidity form of *A. capillus* extract (see Fig. 2).

Moreover, a band at 2927 cm^{-1} was described to the aliphatic C–H groups beside the chain in the structure. Nearby 1612 cm^{-1} band matches to C=O stretching vibration, whereas the 1408 and 1054 cm^{-1} bands corresponds to the symmetric bending of CH and NH_2 groups respectively. The lifted one at 1284.59 cm^{-1} is credited to the C–H bending form in the alkanes. The FTIR method confirms the reduction of Selenium. As the bands at 711.73 and 530.42 cm^{-1} refer to the binding of SeNPs with the hydroxyl groups as Se–O which indicates the coordination bonds between chemical constituents of *Adiantum capillus* extract and Selenium.

The other peak shifted from 1384.89 cm^{-1} to 1451.24 cm^{-1} specifies the SeNPs formation by reduction of carbonyl groups of *A. capillus* extract. Also peaks shifted from 1010.70 cm^{-1} to 1031.92 cm^{-1} and loss of 3377.36 cm^{-1} peak indicates that ether, alkanes, alcohols and esters involvement in the selenium nanoparticles capping procedure as shown in Fig. 2a. Various peaks were seen from *A. capillus* extract between 4000 and 400 cm^{-1} analo-

Table 1
The effect of *Adiantum capillus* crude extract and its synthesized SeNPs on kidney function tests.

Groups	Blood Urea	BUN	Creatinine	Uric Acid	Serum Protein	Serum Albumin
Gen.	61.66 ± 0.33 ^a	59 ± 5.7 ^a	1.93 ± 0.36 ^a	6.43 ± 0.35 ^a	2.9 ± 0.3 ^a	1.57 ± 0.26 ^a
N.	22.67 ± 0.88 ^b	25.0 ± 1.5 ^b	0.47 ± 0.009 ^b	1.33 ± 0.41 ^b	6.6 ± 0.12 ^b	3.93 ± 0.03 ^b
AcLD	36.67 ± 2.3 ^c	32.33 ± 0.67 ^c	0.66 ± 0.05 ^c	4.43 ± 0.03 ^c	4.97 ± 0.18 ^c	2.37 ± 0.09 ^c
AcHD	39.67 ± 0.33 ^c	34.0 ± 2.3 ^c	0.52 ± 0.003 ^c	4.53 ± 0.12 ^c	4.93 ± 0.09 ^c	2.37 ± 0.12 ^c
SnLD	24.33 ± 2.4 ^b	18.33 ± 2.3 ^b	0.47 ± 0.032 ^b	1.83 ± 0.15 ^b	6.03 ± 0.03 ^b	3.43 ± 0.23 ^b
SnHD	21.0 ± 2.1 ^b	15.33 ± 1.2 ^b	0.38 ± 0.02 ^b	1.57 ± 0.18 ^b	6.0 ± 0.12 ^b	3.33 ± 0.03 ^b

Data were presented as Mean ± SEM; Significance was set when $P \leq 0.05$, different superscripts indicate significant difference between groups. Gen: Gentamicin, N.: normal saline, AcLD: *Adiantum capillus* low dose, AcHD: *Adiantum capillus* high dose, SnLD: Selenium nanoparticle low dose and SnHD: Selenium nanoparticle high dose.

gous to 1010.7 cm^{-1} –C–O stretch, carboxylic acids, alcohols, ethers, esters; 1649.14 cm^{-1} – C=O stretch, saturated alkanes, aldehydes; and 3377 cm^{-1} – N–H stretch, 10, 20 amines as shown in Fig. 2(a).

3.3. Thermal stability and XRD crystallography analysis

X-ray crystallography technique was performed to recognize the crystalline phase as shown in Fig. 3, shows the planes and the diffraction peaks listed on positions $2\theta = 14.57^\circ$ (111), 32.33° (200), 40.9° (220), 43.36° (102), and 49.12° (112), confirming the occurrence of crystalline form of SeNPs. The deep peak at $2\theta = 32.33^\circ$ (200) illustrate the occurred orientation to the evaluated surface and confirm the high purity of SeNPs that prepared. The mean crystallite size is measured theoretically by the Debye-Scherrer equation:

$$D = \frac{K\lambda}{\beta \cos \theta}$$

As K is the Scherrer constant (0.9), λ is the X-ray wavelength, β is the full width at half point of the XRD peak, and θ is the Bragg angle. Thus, the calculated crystallite particle size is around 37 nm.

3.4. SEM and EDX analysis of SeNPs

EDX spectrum of the biosynthesized SeNPs, confirms the presence of elemental Selenium and oxygen signals (Fig. 4). Elemental microanalysis derived from the synthesized SeNPs indicates the presence of constituent elements like selenium (67.99%), sodium (5.39%), and oxygen (26.62%). This sort of elemental selenium provided in the form of nanoparticles was widely used to prepare antifungal formulations. Other peaks detected for oxygen and sodium may be from the mixed components present in the aqueous *A. capillus* leaf extract. Strong peaks at 1.5, 4.7, 11.2, and 12.5 keV of the EDX spectrum confirm the presence of elemental selenium.

To scrutinize the morphology of the synthesized Nano-selenium, SEM analysis was used. The predominant shape of Nano-selenium is spherical and cubic at different magnification levels (Fig. 5).

The spherical and cubic bulky forms were the predominant form as seen by SEM also at two different magnifications SEM image (Fig. 5a and 5b) showed that the SeNPs were made of spherical and cubic shapes with a narrow size scattering of 22.04–128.43 nm. Moreover, the grains are aggregated due to the nucleation growth and reduction of the reduced atoms. The reason may be due to the occurrence of several functional groups like lignin in an *A. capillus* leaf extract bind and nucleate selenium ions. The more accessible metal ions are involved in fewer nucleation processes, leading to metal agglomeration (see Fig. 5).

3.5. Animal study

The other part of our study was to test the efficacy of crude extract and synthesized nanoparticles from *Adiantum capillus* in experimental rats, results revealed that *Adiantum capillus* crude extract exhibit a protective effect against gentamicin induced kidney toxicity as showed in (Table 1). Significant differences were found between *A. capillus* low dose (100 mg/kg) and high dose (200 mg/kg) groups and gentamicin group; However, mean numbers were still differ significantly with the vehicle group (normal saline). Whereas the both low dose (100 mg/kg) and high dose

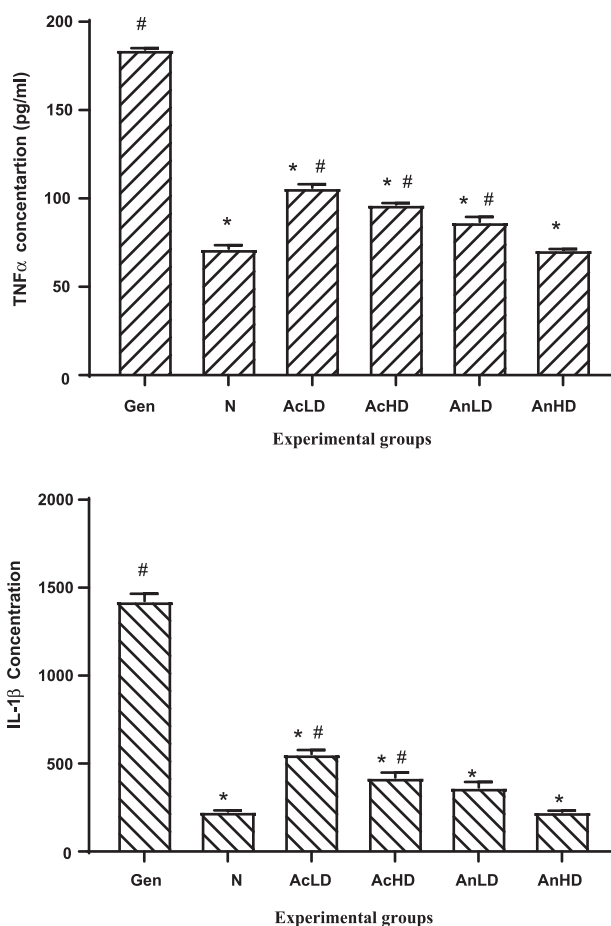


Fig. 6. The concentration of Interleukin-1 beta (IL-1beta) and Tumor necrosis factor alpha (TNF α) in all experimental groups. Gen: Gentamicin, N.: normal saline, AcLD: *Adiantum capillus* low dose, AcHD: *Adiantum capillus* high dose, SnLD: Selenium nanoparticle low dose and SnHD: Selenium nanoparticle high dose. Data presented as mean ± SEM, (*) indicates significance when compared to gentamicin group, (#) indicates significance when compared to the Normal saline group.

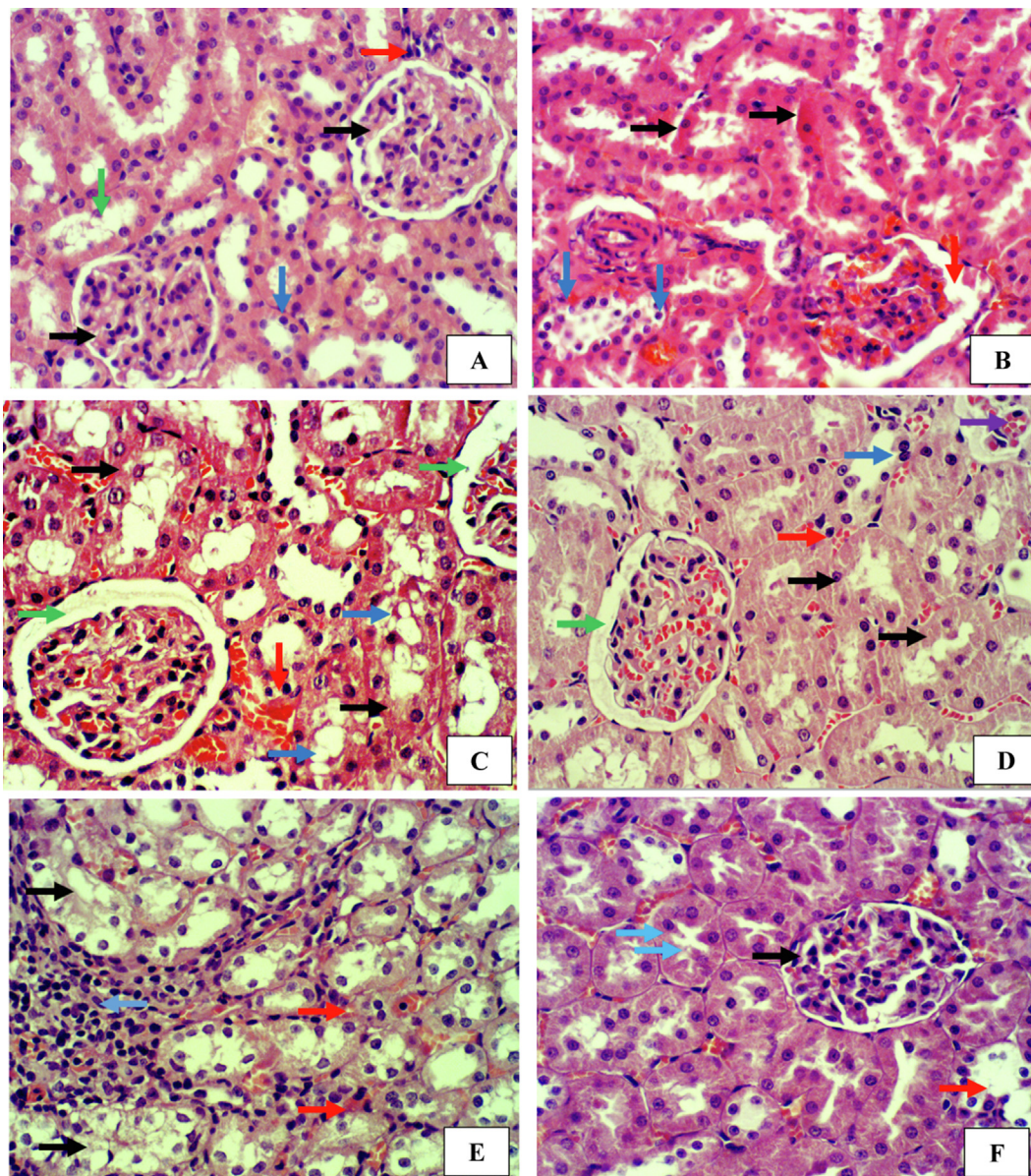


Fig. 7. H&E. 400X. (A) Normal group showed normal histological architectures of glomeruli (Black arrow), proximal convoluted tubules (Blue arrow), distal convoluted tubules (Green arrow), juxtaglomerular complex (Red arrow) (B) Gentamycin group showed cloudy cell swelling (Black arrow), coagulative necrosis in the epithelial cell lining renal tubules (Blue arrow), edema between glomerular tuft and Bowman's capsule (Red arrow). (C) AclD group showed coagulative necrotic epithelial cells lining renal tubules (arrow), sloughing as cellular debris (Blue arrow), interstitial hemorrhages (Red arrow), increase in Bowman's space (Green arrow). AChD group showed few necrotic epithelial cells lining renal tubules (Black arrow), pyknotic nucleus as a first stage of necrosis (Blue arrow), hemorrhages (Red arrow), increase in Bowman's space (Green arrow), congestion in subcapsular venule (Purple arrow). (E) SnLD group showed few necrotic collecting tubules (Black arrow), infiltration of inflammatory cells especially lymphocytes (Blue arrow), with interstitial hemorrhages (Red arrow). (F) SnHD group showed normal histological architectures of glomerular tuft (Black arrow), normal proximal convoluted tubules (Blue arrow), congestion in afferent blood vessel (Red arrow).

(200 mg/kg) of synthesized selenium nanoparticle groups showed comparable results to that of vehicle group and are significantly differ than the gentamicin group (Table 1).

3.6. Detection of interleukin- β 1 and tumor necrosis factor- α

To prove the therapeutic effectiveness of the samples used on another way, the rat's immune response was tested by measuring the pro-inflammatory cytokines interleukin beta (IL- β) and tumor necrosis factor alpha (TNF- α) levels in their sera. Results in Fig. 6 shows that rats injected with gentamicin elevated the cytokines titration to a significant level when compared to the vehicle group

(Normal saline group) but treatment with crude extract of *Adiantum capillus* decreased these levels however synthesized selenium nanoparticles showed the best results in which the levels were near to their normal titration in the vehicle group.

3.7. Histopathological analysis and immunohistochemistry

Histopathological survey of kidney tissues displayed that eight days treatment with gentamicin caused strong signs and marks of nephrotoxicity which represented as necrosis and oedema (Fig. 7/B) while treatment with crude extract of *Adiantum capillus* exhibited similarly toxic effects like haemorrhage and sloughing

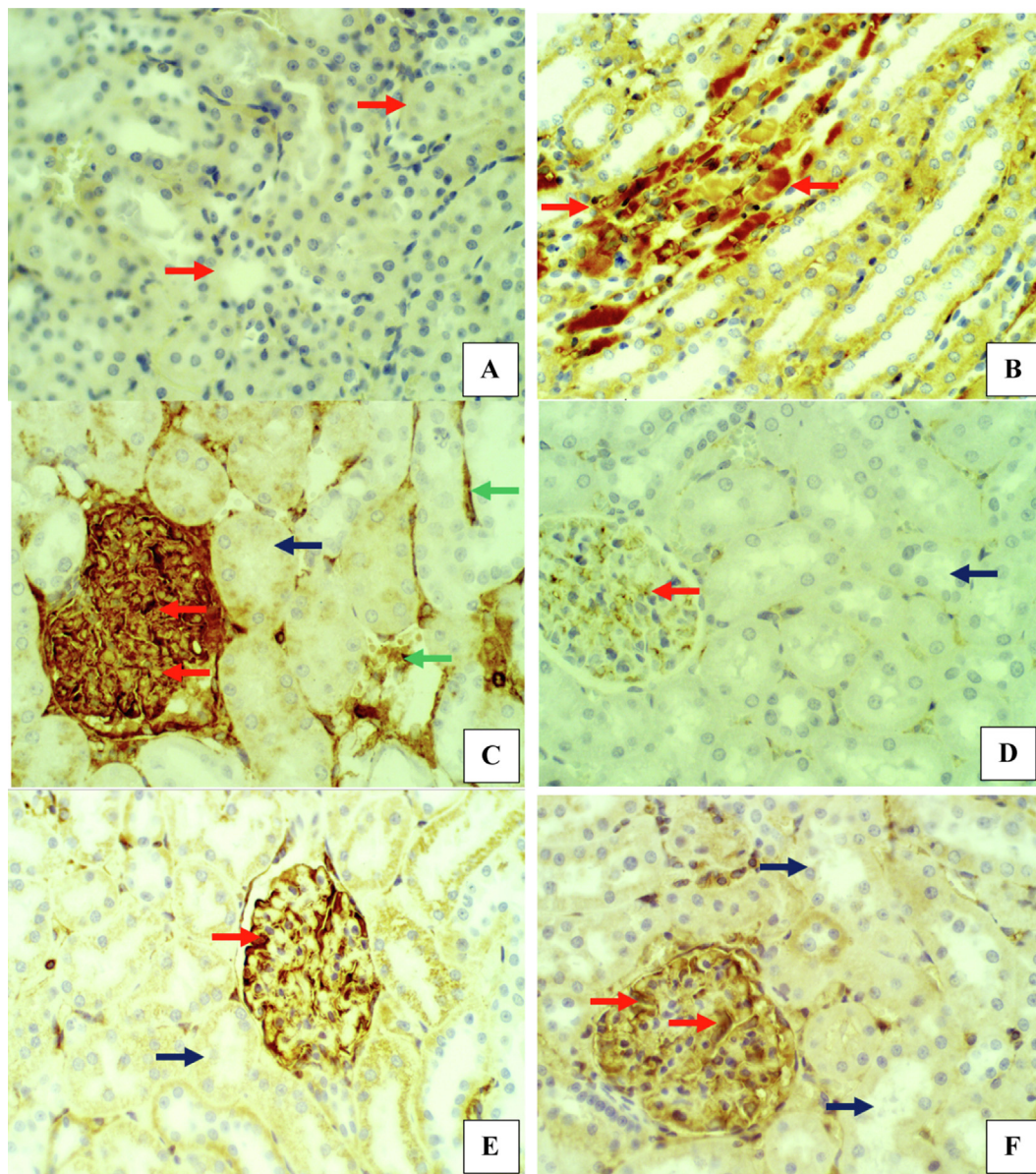


Fig. 8. IHC *Bcl2*-ab. 400x. (A) Normal Saline group. Showed negative staining with *Bcl2* antibodies in the renal tubules (Red arrow). (B) Gentamycin group. Showed epithelial cells in renal tubules have high positive reaction of *Bcl2* that present as cytoplasmic gold dark brown coloration (Red arrow). (C) AcLD group. Showed very strong positive staining to *Bcl2* antibodies in glomerular tuft as a cytoplasmic golden brown patch (Red arrow), with negative reacting was observed in other renal tubules (Black arrow), notice unspecific reacting in extracellular matrix (Green arrow). (D) AChD group. Showed weak positive staining with *Bcl2* antibodies in few cell in glomerular tuft as a cytoplasmic golden brown patches (Red arrow), with negative reacting was observed in other renal tubules (Black arrow). (E) SnLD group. Showed strong positive staining with *Bcl2* antibodies in few collecting tubules as a cytoplasmic golden brown patches (Red arrow), with negative staining to renal tubules (Black arrow). (F) SnHD group. Showed positive staining with *Bcl2* antibodies in the glomerular tuft as a cytoplasmic golden brown patches (Red arrow), and negative staining to *Bcl2* antibodies in the renal tubules (Black arrow).

of cells as showed in (Fig. 7 C&D). Oppositely, kidney tissues of rats treated with synthesized selenium nanoparticle showed normal histological architecture analogous to the normal group.

On the other hand, *Bcl-2* protein expression was evidently increased in the gentamicin treated rats kidney tissues (strong staining of the *Bcl-2* protein), (Fig. 8/B) as compared to the normal group rats kidney tissues (negative staining of the protein), (Fig. 8/A). However, treatment with *Adiantum capillus* crude extract doses showed different results as it was strong positive for low dose group and weak positive for high dose group which indicate the beginning of the recovery. The synthesized nanoparticle treated rat's kidney tissues showed positive staining in few areas and negative staining on the other areas. (Fig. 8 C&D).

Moreover, to predict the renal fibrosis the Vimentin protein expression was screened as well, kidney tissues of vehicle treated group expressed negative staining of that protein and oppositely gentamicin treated rat's kidney tissues expressed strong vimentin staining whereas positive staining was showed by *Adiantum capillus* crude extract groups, Weak positive and negative vimentin staining results were given by selenium nanoparticles groups respectively (Fig. 9).

4. Discussion

Plant extracts have been used as therapeutic agents and being important for human health worldwide for long times. Recently,

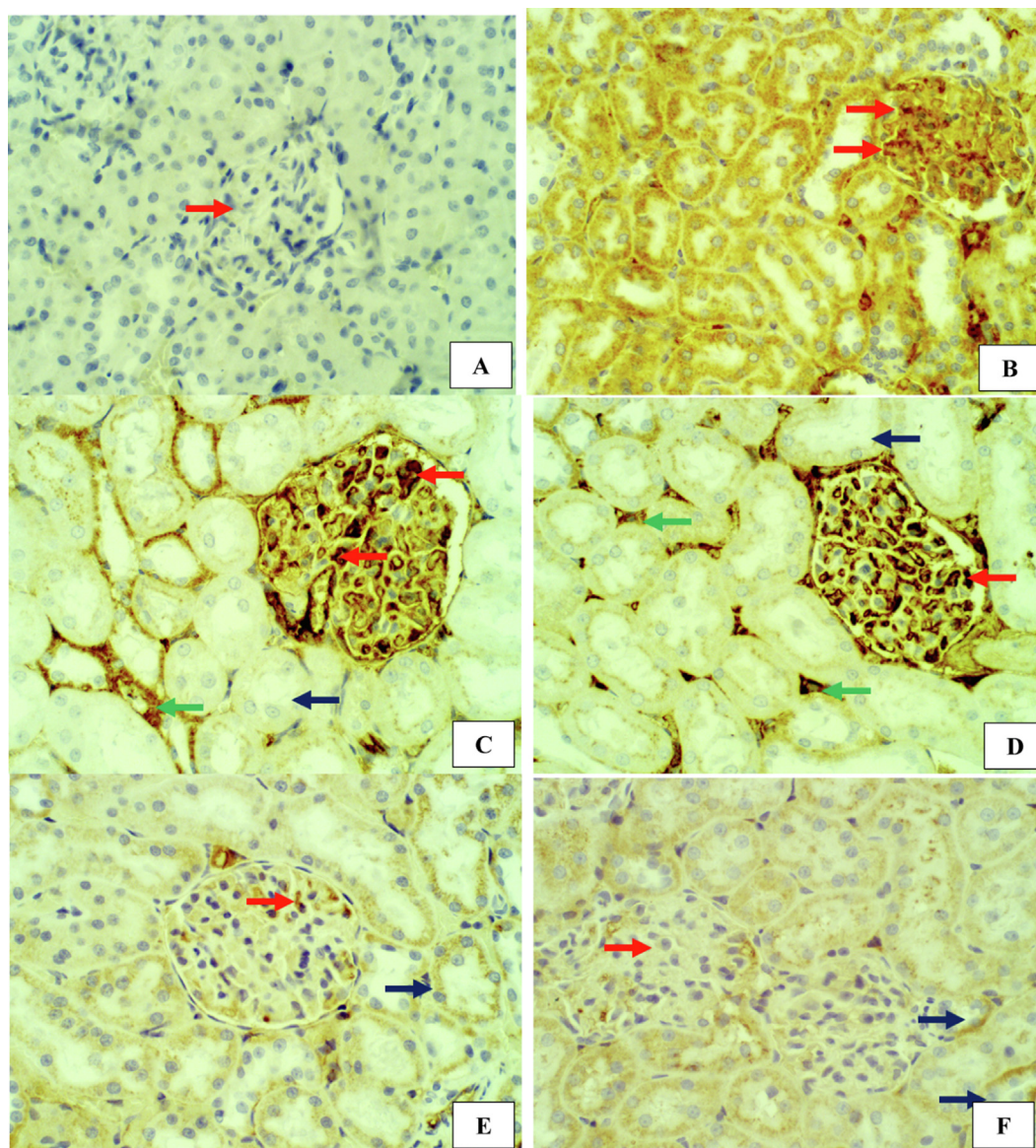


Fig. 9. IHC *Vimentin* -ab. 400x. (A) Normal group showed negative staining with *Vimentin* antibodies in the glomerular tuft (Red arrow). (B) Gentamycin group showed glomerular tuft have high positive reaction of *vimentin* that present as cytoplasmic gold brown coloration (Red arrow). (C) AcLD group showed positive staining with *Vimentin* antibodies in the glomerular tuft as cytoplasmic patches golden brown stain (Red arrow), negative staining in the proximal convoluted (Blue arrow), notice unspecific staining in the extracellular matrix (Green arrow). (D) AcHD group showed positive staining with *Vimentin* antibodies in the glomerular tuft as cytoplasmic granular golden brown stain (Red arrow), negative staining in the proximal convoluted (Blue arrow), notice unspecific staining in the extracellular matrix (Green arrow). (E) SnLD group showed few weak positive staining with *Vimentin* antibodies in the glomerular tuft (Red arrow), and weak positive staining in other renal tubules (Blue arrow). (F) SnHD group showed negative staining with *Vimentin* antibodies in the glomerular tuft (arrow), and weak positive staining in the proximal convoluted tubules in few of them (Blue arrow).

it has been an excessive challenge for the researchers to develop new products from plant and microorganisms as biological sources of products with potential benefits. Nanoparticles synthesized from plant origins have been proven to be environmentally benign (Mittal et al., 2013), the synthesis process is more stable and are more pharmacologically active than chemo-physically produced nanoparticles (Singh et al., 2016). Also the synthesis of nanoparticles from plant extracts has less destructive effects when compared with the other laboratory and industrial methods of their synthesis (Singh et al., 2018). In this study, results demonstrated that The UV-Vis and FTIR spectrometry of *Adiantum capillus* leaf extract certified that this plant extract is a candidate to synthesize SeNPs. The XRD spectrum and the SEM images confirmed the crystallography, the spherical and cubic shapes of the particles. Moreover, strong peaks were observed at 1.5, 4.7, 11.2, and 12.5 keV of

the EDX spectrum confirm the presence of elemental selenium. These properties of the synthesized SeNPs affect the biological activity of it that represented in this study through the protective effect against gentamicin induced toxic effects to the kidneys of rats. Essentially, kidney has an important function to maintain the metabolic activity. Hence, it is critical to analyze the kidney function through evaluating blood urea, total protein, creatinine, BUN, total albumin, and uric acid levels in the serum. Remarkably, the treatment with SeNPs recovers kidney function tests, suggesting that SeNPs won't cause nephrotoxicity. Data in Table 1 showed that the crude extract exhibit protective role when compared the gentamicin group but the results were significantly more protecting for the synthesized SeNPs groups. The pro-inflammatory cytokines levels confirm the protective role of the synthesized SeNPs in which the titration of interleukin-beta and tumor necrosis

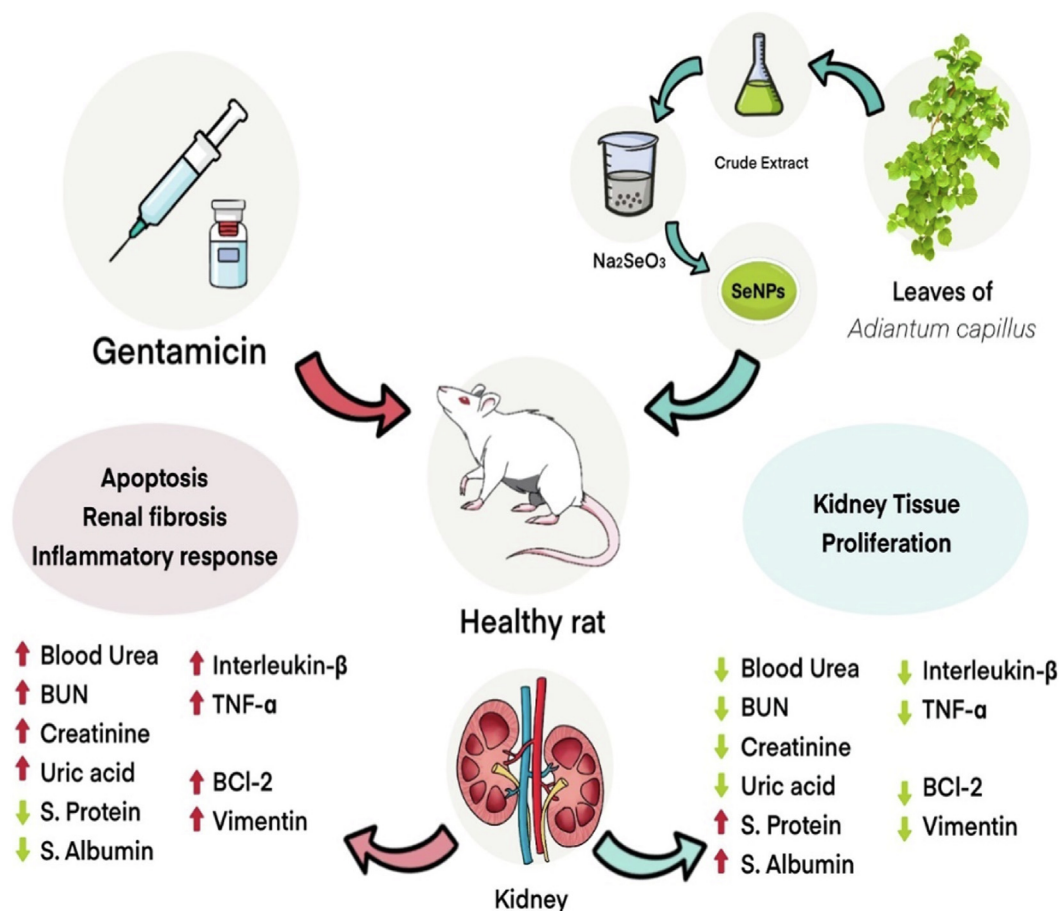


Fig. 10. The suggested mechanism of *Adiantum capillus* nephroprotective action.

factor alpha levels were resumed to their normal levels after treatment with the low dose and high dose of the nanoparticle groups and these results were significantly better than the *Adiantum capillus* crude extract treated groups. Several studies reported the role of cytokines like interleukin-1, tumor necrosis factor alpha, transforming growth factor beta, platelet-derived growth factor and other cytokines on the proliferation of renal interstitial fibroblast cell lines taken from kidney biopsies with interstitial fibrosis and glomerulonephritis. They suggested that the role of these cytokines may differ in acute and chronic inflammatory responses. In acute inflammatory response, kidney pro-inflammatory cytokines may cause apoptosis of interstitial fibroblasts though in chronic response, cytokines may induce proliferation (Lonnemann et al., 1995).

Bcl-2 family members are proto-oncogenes that impact apoptosis. Overexpression of it raises the cells viability under contrary conditions like loss of cell adhesion, cytokine withdrawal, also γ -irradiation. Changes in the Bcl-2 family member's expression may perhaps influence the differentiation state (Sorenson, 2004). In this study, only the vehicle group showed a negative staining for Bcl-2 protein while the other groups showed variable staining impacts that's because this protein exist and remain inside the renal cells till the causing stress is de-activated and another reason is that BCL-2 proteins control renal cell housekeeping roles including autophagy, cell metabolism, mitochondrial biogenesis and mitochondrial morphology (Borkan, 2016). A similar study has reported that selenium element performed a protective effect through regulating the apoptosis, reducing oxidative stress and recovering the expression of Bcl-2/caspase family proteins (Gao et al., 2021).

In like manner, Vimentin protein is expressed mainly at the cytoskeleton and it is a marker of regeneration and tubule-interstitial damages. In kidneys the expression of vimentin defines renal injury in different conditions like [ureteral obstruction](#), severe proteinuria, aging and [Adriamycin nephropathy](#) (Bravo et al., 2003). In this study normal saline group kidney sections showed negative staining of vimentin protein which indicates no injury situation while oppositely treatment with gentamicin displayed strong vimentin staining results which in-turn relates the toxic effects of the drug and supports the previous studies that conform the over expression of vimentin during gentamicin treatment (Francescato et al., 2012). That protein expression was improved in *Adiantum capillus* crude extract treated rats and were much better in SeNPs treated rats which indicate the decrease in the injury level. Finally, a possible mechanism is proposed in Fig. 10 in which, the readjustment of kidney function parameters (blood urea, BUN, creatinine, uric acid, serum protein and serum albumin) along with the regulation of the inflammatory response represented as expression of IL-1 β , TNF- α together with the presence of Bcl-2 and Vimentin proteins in kidney sections suggest the protective effect of SeNPS through regulating apoptosis, providing cell resistance and bypassing their hurts.

5. Conclusion

Selenium nanoparticles synthesized from *Adiantum capillus* plant extract exhibited protective effect against gentamicin induced nephrotoxicity in rats. This can be used in various biomedical applications related to cancer diagnostics and therapeutics for

the benefit of human civilization. Additionally, less costly and eco-friendly procedures comparable to the traditional methods of nanoparticles production need to develop. Also more biological activities need to be addressed to prove their safety, biocompatibility and bioavailability.

Funding

This research did not receive any specific grant from funding agencies in the public, commercial, or not-for-profit sectors.

Declaration of Competing Interest

The authors declare that they have no known competing financial interests or personal relationships that could have appeared to influence the work reported in this paper.

References

- Albus, U. 2012. Guide for the Care and Use of Laboratory Animals. In: Research IFLA, editor. 8th Edition ed. USA: SAGE Publications Sage UK: London, England; 2012. p. 246.
- Ali, B., 2004. The effect of *Nigella sativa* oil on gentamicin nephrotoxicity in rats. *Am. J. Chin. Med.* 32 (01), 49–55.
- Ananth, A., Keerthika, V., Rajan, M.R. 2019. Synthesis and characterization of nano-selenium and its antibacterial response on some important human pathogens. *Current Science* (00113891). 116(2).
- Bledsoe, G., Crickman, S., Mao, J., Xia, C.-F., Murakami, H., Chao, L., et al., 2006. Kallikrein/kinin protects against gentamicin-induced nephrotoxicity by inhibition of inflammation and apoptosis. *Nephrol. Dial. Transplant.* 21 (3), 624–633.
- Borkan, S.C. (Ed.), 2016. The role of BCL-2 family members in acute kidney injury. *Seminars in Nephrology*. Elsevier.
- Bravo, J., Quiroz, Y., Pons, H.C., Parra, G., Herrera-Acosta, J., Johnson, R.J., et al., 2003. Vimentin and heat shock protein expression are induced in the kidney by angiotensin and by nitric oxide inhibition. *Kidney Int.* 64 (86), S46–S51.
- Cao, L., Zhi, D., Han, J., Kumar Sah, S., Xie, Y., 2019. Combinational effect of curcumin and metformin against gentamicin-induced nephrotoxicity: Involvement of antioxidative, anti-inflammatory and antiapoptotic pathway. *J. Food Biochem.* 43 (7), e12836.
- Cittrarasu, V., Kaliannan, D., Dharman, K., Maluventhen, V., Easwaran, M., Liu, W.C., et al., 2021. Green synthesis of selenium nanoparticles mediated from *Ceropegia bulbosa* Roxb extract and its cytotoxicity, antimicrobial, mosquitocidal and photocatalytic activities. *Sci Rep.* 11 (1), 1032.
- Erseçkin, V., Mert, H., İrak, K., Yildirim, S., Mert, N., 2020. Nephroprotective effect of ferulic acid on gentamicin-induced nephrotoxicity in female rats. *Drug Chem. Toxicol.*, 1–7.
- Francescato, H., Chierice, J., Marin, E., Cunha, F., Costa, R., Silva, C., et al., 2012. Effect of endogenous hydrogen sulfide inhibition on structural and functional renal disturbances induced by gentamicin. *Braz. J. Med. Biol. Res.* 45 (3), 244–249.
- Gao, J., Tian, X., Yan, X., Wang, Y., Wei, J., Wang, X. et al. 2021. Selenium Exerts Protective Effects Against Fluoride-Induced Apoptosis and Oxidative Stress and Altered the Expression of Bcl-2/Caspase Family.
- Han, X., Qin, P., Li, W., Ma, Q., Ji, C., Zhang, J., et al., 2017. Effect of sodium selenite and selenium yeast on performance, egg quality, antioxidant capacity, and selenium deposition of laying hens. *Poult. Sci.* 96 (11), 3973–3980.
- Ince, S., Kucukkurt, I., Demirel, H.H., Arslan-Acaroz, D., Varol, N., 2020. Boron, a trace mineral, alleviates gentamicin-induced nephrotoxicity in rats. *Biol. Trace Elem. Res.* 195 (2), 515–524.
- Kim, B.-Y., Jang, S.-Y., Choi, D.-H., Jung, C.-H., Mok, J.-O., Kim, C.-H., 2021. Anti-inflammatory and antioxidant effects of selenium on orbital fibroblasts of patients with Graves ophthalmopathy. *Ophthalm. Plast. Reconstr. Surg.* 37 (5), 476–481.
- Lipinski, B., 2017. Sodium selenite as an anticancer agent. *Anti-Cancer Agents in Medicinal Chemistry (Formerly Current Medicinal Chemistry-Anti-Cancer Agents)*. 17 (5), 658–661.
- Lonnemann, G., Shapiro, L., Engler-Blum, G., Müller, G.A., Koch, K.M., Dinarello, C.A., 1995. Cytokines in human renal interstitial fibrosis. I. Interleukin-1 is a paracrine growth factor for cultured fibrosis-derived kidney fibroblasts. *Kidney Int.* 47 (3), 837–844.
- Lv, L., Zhang, H., Liu, Z., Lei, L., Feng, Z., Zhang, D., et al., 2020. Comparative study of yeast selenium vs. sodium selenite on growth performance, nutrient digestibility, anti-inflammatory and anti-oxidative activity in weaned piglets challenged by *Salmonella typhimurium*. *Innate Immun.* 26 (4), 248–258.
- Mittal, A.K., Chisti, Y., Banerjee, U.C., 2013. Synthesis of metallic nanoparticles using plant extracts. *Biotechnol. Adv.* 31 (2), 346–356.
- Pfister, C., Dawczynski, H., Schingale, F.-J., 2016. Sodium selenite and cancer related lymphedema: Biological and pharmacological effects. *J. Trace Elem. Med Biol.* 37, 111–116.
- Pyrzynska, K., Sentkowska, A., 2021. Biosynthesis of selenium nanoparticles using plant extracts. *Journal of Nanostructure. Chemistry*.
- Randjelovic, P., Veljkovic, S., Stojiljkovic, N., Sokolovic, D., Ilic, I., 2017. Gentamicin nephrotoxicity in animals: Current knowledge and future perspectives. *EXCLI J.* 16, 388.
- Salari, S., Bahabadi, S.E., Samzadeh-Kermani, A., Yosefzadei, F., 2019. In-vitro evaluation of antioxidant and antibacterial potential of greensynthesized silver nanoparticles using *Prosopis farcta* fruit extract. *Iranian journal of pharmaceutical research: IJPR.* 18 (1), 430.
- Shi, L., Xun, W., Yue, W., Zhang, C., Ren, Y., Shi, L., et al., 2011. Effect of sodium selenite, Se-yeast and nano-elemental selenium on growth performance, Se concentration and antioxidant status in growing male goats. *Small Rumin. Res.* 96 (1), 49–52.
- Shoebi, S., Mashreghi, M., 2017. Biosynthesis of selenium nanoparticles using *Enterococcus faecalis* and evaluation of their antibacterial activities. *J. Trace Elem. Med Biol.* 39, 135–139.
- Singh, J., Dutta, T., Kim, K.-H., Rawat, M., Samddar, P., Kumar, P., 2018. 'Green'synthesis of metals and their oxide nanoparticles: applications for environmental remediation. *Journal of nanobiotechnology.* 16 (1), 1–24.
- Singh, P., Kim, Y.-J., Zhang, D., Yang, D.-C., 2016. Biological synthesis of nanoparticles from plants and microorganisms. *Trends Biotechnol.* 34 (7), 588–599.
- Sorenson, C.M., 2004. Bcl-2 family members and disease. *Biochimica et Biophysica Acta (BBA)-Molecular. Cell Res.* 1644 (2–3), 169–177.
- Wu, X., Zhao, G., He, Y., Wang, W., Yang, C.S., Zhang, J., 2019. Pharmacological mechanisms of the anticancer action of sodium selenite against peritoneal cancer in mice. *Pharmacol. Res.* 147, 104360.